

## **Electrochemical Impedance Response of Zn and Galvanized Steel Corroding under Marine Atmospheric Environments**

**Amar Prasad Yadav\***

*Department of Metallurgy and Ceramics Sci., Tokyo Institute of Technology, Tokyo, Japan.  
e-mail: [amar2y@yahoo.com](mailto:amar2y@yahoo.com)*

### **Abstract**

*Impedance response of zinc and galvanized steel samples exposed in wet-dry cyclic condition using 0.05 M NaCl solution has been analyzed in order to evaluate their corrosion behavior. The wet-dry cyclic test was performed by exposing sample to alternate conditions of 1 h immersion in 0.05 M NaCl solution and 7 h drying at 298 K with relative humidity (RH) of 60% for 10 days consisting of 30 cycles. After initial exposure to corrosion test, samples showed the evolution of two capacitive loops. However, a sharp decrease of characteristic frequency, characterized by an increase of double layer capacitance in the range of several  $\text{mF}/\text{cm}^2$ , with the progress of corrosion was observed. This was explained by taking into account the coupling of characteristic frequencies of the two capacitive loops due to deposition of thick layer of porous rust. The parameters of diffusion impedance for the cathodic process were estimated from the low frequency capacitive loops attributed to finite Warburg diffusion impedance. A sharp increase of impedance after several days of corrosion in the case of galvanized steel was attributed to the dissolution of Fe-Zn alloy layer that is formed during galvanizing process.*

**Keywords:** *galvanized steel, zinc, atmospheric corrosion, wet-dry cyclic test.*

### **Introduction**

The kinetics of the zinc electrochemical reactions have been the subject of many publications.<sup>1-5</sup> The dissolution mechanism of zinc has been extensively studied in acidic and alkaline medium in both complexing and noncomplexing solutions.<sup>6,7</sup> In acidic or around neutral solutions, the accepted dissolution mechanism involves two-step charge transfer reactions as;

---

\* **Corresponding author** & present address: Central Department of Chemistry, Tribhuvan Univ., Nepal

However, this scheme cannot explain the presence of several low frequencies capacitive-inductive loops observed in the ac impedance spectra. A more complex reaction model with two competitive parallel reaction paths of dissolution including a catalytic step has been reported in deaerated  $\text{ZnCl}_2\text{-NH}_4\text{Cl}$  medium.<sup>8,9</sup> Furthermore, the same model was applied quite satisfactorily to the aerated sulfate solution with the modification of cathodic reduction of hydrogen by oxygen.<sup>5</sup> However, all these studies have been made at current densities higher than few  $\text{mA cm}^{-2}$ . In the vicinity of rest potential, very small current flows and the surface state changes rapidly. These are related to the presence of oxide film, which is easily formed on reactive metals like zinc during polishing.



When exposed to wet-dry cyclic marine environments, both zinc and galvanized steel have shown to corrode with the formation of porous and non-adherent corrosion products, which makes it difficult to interpret the evolution of impedance spectra with time.<sup>10</sup> In this context, the electrochemical impedance spectroscopy (EIS) is used to record the impedance response of bulk zinc and galvanized steel corroding under wet-dry cyclic environment. This work is aimed to interpret the time evolution of impedance response of zinc and galvanized steel so as to understand the corrosion process under wet-dry cyclic environments.

## **Experimental Methods**

Commercial hot-dip galvanized steel (GI) with the coating thickness of about  $8.5 \mu\text{m}$  and bulk zinc with 99.99% purity were used as the test materials. For the measurement of electrochemical impedance, a two-electrode cell arrangement with the exposed area of  $10 \text{ mm}^2$  each was used as shown in Fig.1. One metal plate was served as the working electrode and other as the counter electrode, and they were mounted face to face in an ambient temperature solidifying resin with the separation gap of 0.1 mm. The gap between two metal sheets was covered with a thin layer of epoxy to avoid possible crevice corrosion and to prevent the coupling due to deposition of the corrosion products.<sup>11</sup> In the case of zinc sample, before embedding it in the epoxy, it was subjected to electro-deposition coating employing an organic resin for 3 min, which was followed by curing at 443 K for 20 min.

The samples embedded in the epoxy resin were subjected to wet-dry cyclic corrosion test conducted by exposing the samples to an alternate condition of 1 h immersion in 0.05 M NaCl solution and 7 h drying in a chamber set at 298 K and 60% RH using the methods described elsewhere.<sup>10</sup>

The whole frequency impedance response of zinc and galvanized steel samples were measured once a day during immersion condition of the wet-dry cycle.

However, only the impedance responses for 1<sup>st</sup> (8 h), 3<sup>rd</sup> (1 day), 9<sup>th</sup> (3 days), 18<sup>th</sup> (6 days) and 30<sup>th</sup> (10 days) cycle exposure were evaluated. The EIS measurement was carried out using a frequency response analyzer. The impedance spectra were recorded in the frequency range between 10 kHz and 10 mHz. The Z-view software (version 2.6b) was used for evaluating the impedance spectra.

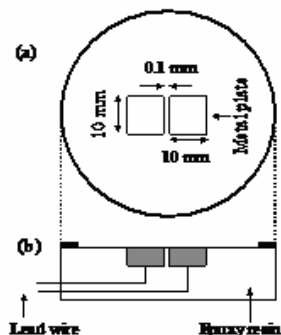


*Figure 1: Schematic showing the two-electrode cell used for corrosion monitoring under wet-dry cyclic condition, (a) the top view and (b) transverse cross sectional view.*

Impedance characteristics of zinc and galvanized steel in the early stage of immersion were also recorded to understand the corrosion process. To provide better accuracy during the frequency sweep, the low frequency limit of the current resistor was set to a fix range after several trials. To support the EIS results, SEM-EDX was used to analyze the cross-section of corrosion products.

## **Results and Discussion**

### *Impedance characteristics under wet-dry cyclic exposure*

The results of impedance measurement after 1<sup>st</sup>, 3<sup>rd</sup>, 9<sup>th</sup>, 18<sup>th</sup> and 30<sup>th</sup> cycle exposures in 1 h wet and 7 h dry cyclic test are shown in Figs 2(a) and 2(b) for zinc and galvanized steel, respectively. The impedance spectra were characterized by two depressed capacitive loops expanding towards lower frequencies until 3<sup>rd</sup> cycle exposure in both cases. The capacitive loops are fairly well resolved to obtain the individual time constants. However, two semicircles are no longer separable and a single time constant is obtained after 3<sup>rd</sup> cycle exposure. Besides this, galvanized steel shows a sharp increase of the impedance after 9<sup>th</sup> cycle exposure compared to that observed for zinc.

Before analyzing the shape of impedance spectra is shown in Fig. 2, the impedance response of both zinc and galvanized steel under initial stage of immersion in 0.05 M NaCl is considered. It is noteworthy to mention that surface of both specimens was relatively free from corrosion products during the immersion condition as described in the experimental methods mentioned in this paper.

Figure 3 shows that the general aspect of impedance spectra in both cases is similar showing the presence of capacitive loops at high and medium frequencies, and an inductive loop at low frequency. The appearance of inductive loop shows that the surface was not stable for recording impedance response. The inductive loop, which was reported as a characteristic adsorption type relaxation on zinc and was suppressed by developing surface layer with the increase of immersion time.<sup>5</sup> It is noticeable that the semicircle loops became flattened in relation with the formation of porous layer with the increase of the immersion time.

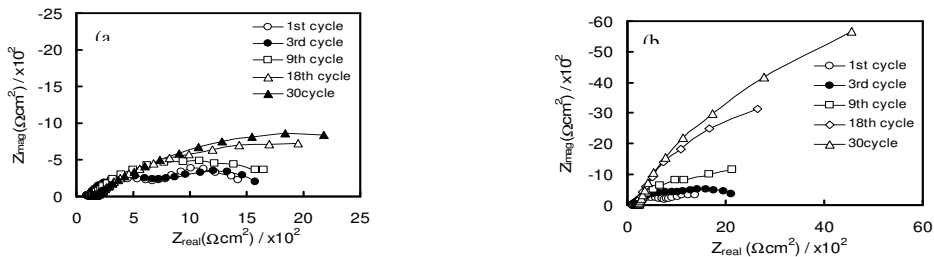
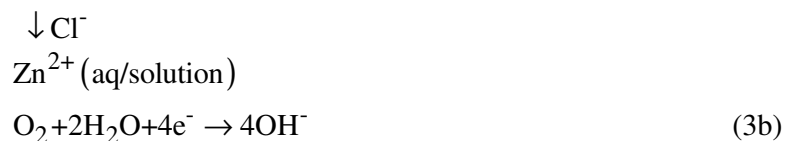
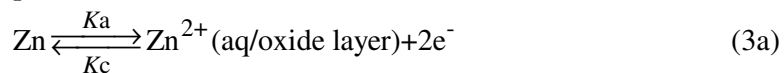


Figure 2: Nyquist plots of impedance response obtained on (a) bulk zinc and (b) galvanized steel exposed under 1 h wet and 7 h dry cyclic conditions.

Figure 3 shows that impedance response is more stable in the case of galvanized coating than bulk zinc probably due to presence of air formed oxide layer on its surface. The impedance is found to decrease (Fig. 3.b, curve 2) in first few hours of immersion in relation with the breakdown of the air formed oxide layer; and then again increased slowly with the formation of corrosion products. After 8 h immersion, the double layer capacitance value, estimated by fitting first capacitive loop, is found to increase from 20 - 66 μF cm<sup>-2</sup> after 15 min immersion of the bulk zinc. On the other hand, it changed from 6 μF cm<sup>-2</sup> after 15 min immersion to 13 μF cm<sup>-2</sup> in the case of galvanized coating layer.

From the results of Fig. 3, it is clear that the porous layer grows on the surface of zinc in the initial stage of corrosion under immersion condition. Accordingly, zinc dissolution occurred through viscous/porous oxide layer, and hence the oxygen reduction proceeded at the solution/oxide interface under diffusion control. The reaction path of zinc corrosion can be written as follows;<sup>12</sup>



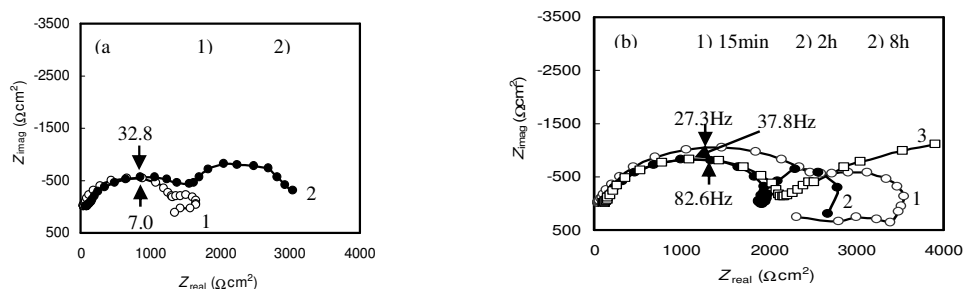


Figure 3: Nyquist plots of impedance response obtained on (a) pure zinc and (b) galvanized steel under initial stage of immersion in 0.05 M NaCl solution.

It is obvious from the impedance response during the initial stage of corrosion in immersion condition that both the samples showed the evolution of two capacitive loops similar to that observed under wet-dry cyclic test. The coupling of the two capacitive loops was noticed only after the electrode surface started to get covered with thick deposit of corrosion products. Therefore, to know the reason for the coupling of two time constants after 3<sup>rd</sup> cycle exposure under wet-dry cyclic exposure, it is important to consider the surface coverage by corrosion products. Figure 4 shows the digital photograph of galvanized steel sample after 3<sup>rd</sup> cycle exposure together with a schematic model showing the influence of rust layer on the oxygen reduction reaction. It is evident that the sample surface is covered with thin and thick layers of corrosion products. It has been observed that the thin and thick layer of rusts have different compositions. Thin layer rust was found to be composed of mainly ZnO and thick layer rust was a mixture of ZnO and ZnCl<sub>2</sub>·4Zn(OH)<sub>2</sub>.<sup>13</sup> In another study, it had reported that the oxygen reduction mechanism on such thin and thick rust layer was different.<sup>11</sup> It had recently found that the ZnO deposited on Pt electrode enhanced the oxygen reduction as compared to a deposit of mixtures of ZnO and ZnCl<sub>2</sub>·4Zn(OH)<sub>2</sub>.<sup>14</sup> This was explained by taking into account the n-type semiconductor nature of ZnO, which helps oxygen reduction on Pt surface by lowering the flat band potential.

From the above discussion, it is proposed that the corrosion will progress at relatively faster rate due to the formation of heterogeneous corrosion products, and hence giving low time constant than the surface covered with thick deposits where corrosion will progress at slow rate due to barrier effect. In such a situation, the two-time constant will be clearly separated, as has been observed until 3<sup>rd</sup> cycle exposure. However, when the surface get covered with a thick corrosion product layer, the respective time constant for charge transfer and diffusion process will increase. This increase of time constant of both the process could lead to the merging of two capacitive loops. To make this explanation more clear, the effect of rust layer on the evolution of individual time constant is discussed in next section.

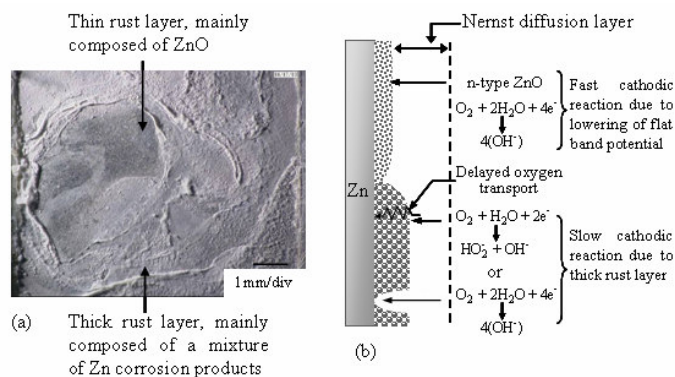


Figure 4: Digital photographs of galvanized steel after 3<sup>rd</sup> cycle exposure in a wet-dry cyclic test in 0.05 M NaCl. A schematic model showing dependence of oxygen reduction rate on the rust layer and thickness is also shown together.

#### Fitting of the impedance data

The analysis of impedance spectra in the initial stage of corrosion has revealed a contradiction between the simultaneous increase of charge transfer resistance and capacitance value with the progress of corrosion. It had reported that the coverage of by a thick surface layer of corrosion product made the impedance spectra more difficult.<sup>10</sup> In this context, an attempt is made to analyze the observed shape of impedance spectra by fitting with a suitable equivalent circuit as shown in Fig. 5. It consists of a solution resistance,  $R_{\Omega}$  in series with a parallel combination of charge transfer resistance,  $R_{ct}$  and constant phase element, CPE. The first capacitive loop is assigned to the charge transfer reaction,  $R_{ct}$ . The second capacitive loop is assigned to the diffusion limited cathodic reduction of oxygen.

From the shape of the second loop a generalized finite length Warburg element  $Z_w$  is included in series with  $R_{ct}$  to account for mass transport contribution. The use of  $Z_w$  is justified since the corrosion rate of zinc and galvanized steel is purely diffusion controlled at or near the corrosion potential. At the same time, it is shown in the previous section of this paper (Fig. 3) that the second capacitive loop enlarged in relation to the formation of porous layer with the elapse of time. Under such condition, the diffusion of oxygen to the electrode surface had determined the rate of reaction.<sup>2,11,15</sup>

Due to frequency dispersion of impedance, the constant phase element approach has been used to fit the data. The fitting has been done from 10 kHz to 1 mHz frequency for all the results and fitting results for 1<sup>st</sup> and 30<sup>th</sup> cycle exposure as shown in Fig. 6. The points in the plots are the experimental values, while the lines are the results of curve fitting. A very good agreement between the experimental value and fitting line is evident. At this point it is important to consider the merging of two-capacitive loops after 3<sup>rd</sup> cycle exposure. As can be seen from Fig. 6, a good

fitting is obtained even if only one time constant is obvious after 9<sup>th</sup> cycle exposure. It is well known that the corrosion of iron in neutral chloride solution is controlled by diffusion of oxygen as well. However, the EIS response never shows diffusion impedance. The reason is that the rate of oxygen diffusion on iron surface without rust or with rust is very high compared to the one on zinc surface. Therefore, the time constant for the appearance of diffusion impedance is very low and only response from charge transfer reaction is obtained.

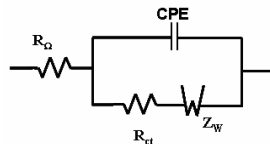


Figure 5: Equivalent circuit of corroding zinc and galvanized steel under wet-dry cyclic exposure.

On the other hand, in the case of zinc it strongly depends on the surface state. For example, when impedance was measured just after 15 min immersion of polished zinc sample, only a very small second semicircle loop due to diffusion is obtained as shown in Fig. 3(a). A schematic model showing the behavior of current-potential with the deposition of corrosion product is shown in Fig. 6(c). In the initial stage, two-time constant can be obtained depending on the amount of rust layer. However, the rate of oxygen diffusion had decreased due to barrier effect and the charge transfer resistance became very high with the deposition of rust.<sup>11</sup> This increased the time constant of the charge transfer reaction, and hence the second semicircle loop disappeared.

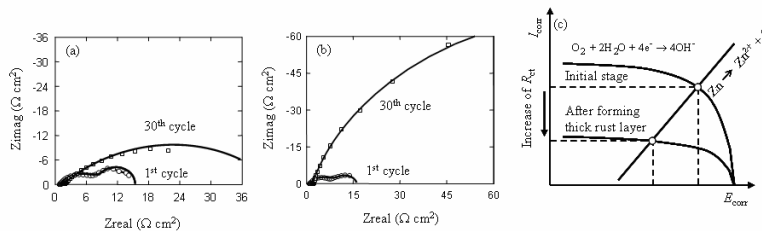


Figure 6: Comparison of measured and simulated impedance diagram obtained using equivalent circuit in (a) pure zinc and (b) galvanized steel. A schematic diagram of the current-potential plot is also shown for zinc (c).

The parameters used for evaluating the impedance diagram are tabulated in Table 1 and Table 2 for bulk zinc and galvanized steel, respectively. The fitting of EIS data with two-time constant shows the increase of both  $R_{ct}$  and  $R_w$  with time, therefore justifying the above conclusion.

From Tables 1 and 2, the fitted parameters  $R_{ct}$  and T are the charge transfer resistance and capacitance, respectively, and plotted against the cycle number as shown in Figs 7(a) and (b). The sharp increase in the value of charge transfer resistance in the case of galvanized steel after 9<sup>th</sup> cycle exposure can be seen as

compared to almost no change in the case of zinc sample. The capacitive element though increased in both the cases, the difference can be seen after 9<sup>th</sup> cycle exposure.

The cross sections of samples exposed to the wet-dry cycle for the different periods of time were observed using SEM to clarify the observed differences in the value of  $R_{ct}$  and capacitive element (T) between zinc and galvanized steel samples. Figures 8 and 9 show the SEM micrograph of the rust layer cross-sections of bulk zinc after 9<sup>th</sup> cycle exposure and the SEM micrograph of galvanized steel samples after different cycles exposure, respectively. The results of EDX analyses carried out both at different points and along a line across the cross-section are also reported.

Tables 1 and 2.

Table I Physical constants obtained after fitting the impedance data of bulk zinc.

Exposed cycle	Parameters						
	$R_{\Omega}$	$R_{ct}$ ( $\Omega\text{cm}^2$ )	T ( $\mu\text{Fcm}^2$ )	P	$R_w$ ( $\Omega\text{cm}^2$ )	W-T ( $\mu\text{Fcm}^2$ )	W-P
1	96	375	380	0.73	350	6.5	0.58
3	108	380	400	0.79	365	12	0.48
9	136	650	1700	0.70	400	15	0.3
18	147	750	2000	0.60	800	17	0.3
30	159	950	2000	0.58	1100	20	0.3

Table II Physical constants obtained after fitting the impedance data of galvanized steel.

Exposed cycle	Parameters						
	$R_{\Omega}$	$R_{ct}$ ( $\Omega\text{cm}^2$ )	T ( $\mu\text{Fcm}^2$ )	P	$R_w$ ( $\Omega\text{cm}^2$ )	W-T ( $\mu\text{Fcm}^2$ )	W-P
1	113	380	480	0.72	375	20	0.47
3	173	650	500	0.80	465	9	0.50
9	190	900	3600	0.78	760	20	0.4
18	195	3500	4100	0.86	1500	30	0.4
30	205	6500	2600	0.85	3500	40	0.4

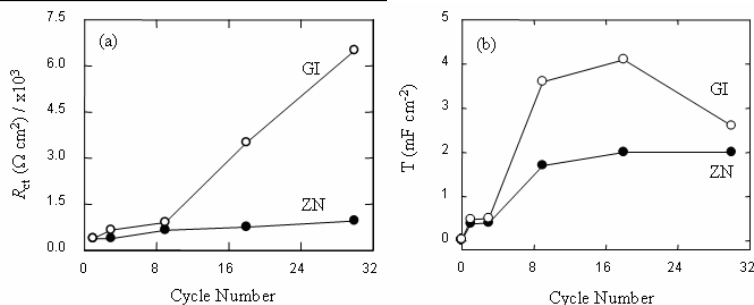


Figure 7: Fitted parameters (a) charge transfer resistance and (b) capacitance of pure zinc and galvanized steel sample.

In the case of bulk zinc, after 9<sup>th</sup> cycle exposure (Fig. 8), a two-layer structure of corrosion products is observed with porous outer layer composed of a mixture of oxide and chloride rich rust while a compact inner layer mainly consisted of oxide rich rust. On the other hand, in the case of galvanized steel after 9<sup>th</sup> cycle exposure (Fig. 9a), a heterogeneous corrosion is observed. The active corrosion is not yet reached to the Zn-Fe alloy layer as can be seen from the results of EDX analysis (point-1, Zn-72.2%, Cl-10.1% and O-15.7% by mass; point-2, Zn-71.3%, Cl-9.7%, O-15% and Fe-32.7% by mass for Fig. 9.a). This suggests that basically both bulk zinc and galvanized steel should show same response to EIS until 9<sup>th</sup> cycle exposure.

Figure 9 (b) shows that the corrosion is reached to the steel substrate of

galvanized steel after 18<sup>th</sup> cycle exposure but corrosion of steel has not yet started. The EDS line analysis was performed along the cross section as shown in Fig. 9.b (point-1, Zn-63.7%, Cl-11.5%, O-15.5% and Fe-7.8% by mass; point-2, Zn-47.7%, Cl-7.6%, O-14.0% and Fe-32.7% by mass). The presence of iron in the centre of the rust layer (point 1) can be related to the beginning of Fe-Zn alloy layer dissolution. Now, it can be assumed that the difference in the EIS response of bulk zinc and galvanized steel after 9<sup>th</sup> cycle exposure can be related to the corrosion of Fe-Zn alloy layer and therefore the presence of iron in the rust after observing the difference in the rust layer composition between bulk zinc and galvanized steel.

Bonnell et al.<sup>17</sup> had reported an abnormal high value of capacitance and had attributed to the porous and conductive nature of underlying deposits. However, in the present study, the simultaneous corrosion of zinc and iron makes it difficult to draw such a conclusion. The reason for the increase of  $R_{ct}$  and capacitive element with the progress of corrosion can be related to the shift of characteristic frequency with the formation of porous corrosion products in combination with the presence of iron rust. It had reported that the Fe-Zn alloy layer had more noble potential than zinc, and hence decreased the corrosion rate.<sup>18,19</sup> A higher value of capacitive element after the dissolution of either alloy layer or iron layer shows the relaxation phenomenon involving iron compounds and therefore a complex nature of the EIS response.

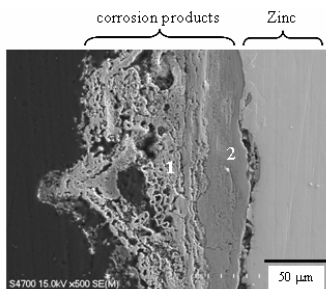


Figure 8: SEM photographs of the cross section of bulk zinc after 18<sup>th</sup> cycle exposure in wet-dry cycles.

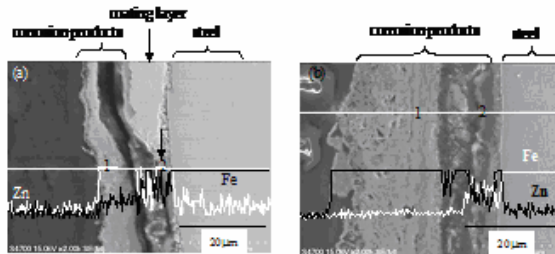


Figure 9: FESEM photographs of the cross section of GI after (a) 9<sup>th</sup> and (b) 18<sup>th</sup> cycles exposure. The EDS line analysis performed along the cross section is also shown.

## Conclusions

This study gives a comparative analysis of EIS response of zinc and galvanized steel corroding under wet-dry cyclic conditions. An approach to fitting the impedance spectra and explaining the abnormal increase of capacitive element has been proposed based on the surface state of the sample, the SEM and EDX analyses of rust layer cross section. The EIS response is complicated by the dissolution of Fe-Zn alloy layer and formation of porous corrosion product, which

decreased the mass transfer of oxidant. Before the commencement of iron corrosion, the impedance response of galvanized coating is similar to that of bulk zinc.

## **References**

1. C. Deslouis, M. Duprat, and C. Tulet-Tournillon; *J. Electroanal. Chem.*, 1984,**181**, 119.
2. L. M. Baugh, *Electrochim. Acta*, 1979,**24**, 657.
3. I. Epelboin, M. Ksouri, and R. Wiart, *J. Electrochem. Soc.*, 1975,**122**,1206.
4. A. E. Bothe, J. R. Vilche, K. Juttner, W. J. Lorenz, W. Kautek, and W. Paatsch, *Corros. Sci.*, 1991,**32**,621.
5. C. Deslouis, M. Duprat, and C. Tournillon, *Corros. Sci.*, 1989,**29**,13.
6. J. O. M. Bockris, Z. Nagy, and A. Danjanovic, *J. Electrochem. Soc.*, 1972,**119**,285.
7. N. A. Hampson, G. A. Herdman, and R. Taylor, *J. Electroanal. Chem.*, 1970,**25**,9.
8. C. Cachet, and R. Wiart, *J. Electroanal. Chem.*, 1980,**111**,235.
9. C. Cachet, and R. Wiart, *J. Electroanal. Chem.*, 1980,**129**,103.
10. A.P. Yadav, A. Nishikata, T. Tsuru, *Corros. Sci.*, 2004,**46**,169.
11. A. P. Yadav, A. Nishikata, T. Tsuru, *J. Electroanal. Chem.*, 2005,**111**,235.
12. L. Sziraki, E. Szocs, Zs. Pilbath, K. papp, and E. Lalman, *Electrochim. Acta*, 2001,**46**,3743.
13. A. P. Yadav, A. Nishikata, T. Tsuru, *Corros. Sci.*, 2004,**46**,361.
14. T. Fujishiro, *Master's Degree Thesis, Tokyo Institute of Technology, Dept. of Metallurgy and Ceramics Science*, (2006).
15. L. Sziraki, A. Cziraki, I. Gerocs, Z. Vertesy and L. Kiss, *Electrochim. Acta*, 1998,**43**,175.
16. B. A. Boukamamp, *Solid State Ionics*, 1980,**20**,31.
17. A. Bonnel, F. Dabosi, C. Deslouis, M. Duprat, M. Keddami and B. Tribollet, *J. Electrochem. Soc.*, 1983,**130**,753.
18. S. E. Hadden, *J. Iron Steel Inst.*, 1952,**6**,121.
19. A. P. Yadav, H. Katayama, K. Noda, H. Masuda, A. Nishikata, T. Tsuru, *Corros. Sci.*, 2007,**49**,3716.